Proceedings of ICMMB-11:
International Conference on Mechanics in Medicine and Biology
April 2-5, 2000 / Maui, Hawaii

2-D SIMULATIONS OF VALVELESS PUMPING USING THE IMMERSED BOUNDARY METHOD

Eunok Jung
Computer Science and Mathematics Division
Oak Ridge National Laboratory

Charles S. Peskin
Courant Institute of Mathematical Science
New York University

ABSTRACT

Flow driven by pumping without valves is examined, motivated by biomedical applications such as cardiopulmonary resuscitation (CPR) and the human fetus before the development of the heart valves. The direction of flow inside a loop of tubing that consists of (almost) rigid and flexible parts is investigated when the boundary of one end of the flexible segment is forced periodically in time. Despite the absence of valves, net flow around the loop may appear in these simulations. The amplitude and even the direction of this flow depend on the driving frequency of the periodic forcing.

INTRODUCTION

Pumping blood in one direction is the main function of the heart, and the heart is equipped with valves that ensure unidirectional flow. Is it possible, though, to pump blood without valves? This paper is intended to show by numerical simulation the possibility of a net flow which is generated by a valveless mechanism in a circulatory system. Simulations of valveless pumping are motivated by the physical experiments of Kilner [3]. He observed net flow in one direction is dependent upon the location of periodic forcing in his model, which is a loop of tubing of which part is almost rigid and the other part flexible. In agreement with Kilner, we find by numerical simulations that net flow can indeed be driven around such a loop by periodic forcing at one location, but we also find something new: the direction of the flow depends on the driving frequency of the periodic forcing.

One of the applications of valveless pumping may be cardiopulmonary resuscitation (CPR). The blood flow during CPR has been explained by two conventional theories: thoracic pump and cardiac compression mechanisms. In the thoracic pump model, it has been reported that the heart is "a passive conduit for blood flow" during chest compression, with an open mitral valve throughout the cardiac cycle and anterograde (forward) transmitral blood flow even during chest compression [1]. However, in the theory of the cardiac pump model, the heart acts as a pump and its valves function normally [2]. Our computational model of valveless pumping may provide assistance in understanding the thoracic pump mechanism. Another biological example of valveless pumping may occur in the human embryo at the end of the third week of gestation. At this stage of development, the valves of the heart have not yet formed. Nevertheless, there is a net flow in the circulatory system that is somehow generated by the beating of the heart. An industrial application of valveless pumping is in microelectromechanical system (MEMS) devices [4], where there is a need to produce fluid motion without moving anything inside the fluid. MEMS devices could be built that incorporate flexible flow channels. In that case, our findings might be applicable to the design of valveless pumps for MEMS devices.

1.Immersed Boundary Method

1.1.Mathematical formulations. The immersed boundary method is applicable to problems involving an elastic structure interacting with a viscous incompressible fluid. It has been applied to a variety of problems, including 3-D simulations of blood flow in the heart [6,7], the design of prosthetic cardiac valves, platelet aggregation during blood clotting, wave propagation in the cochlea, the flow of suspensions, and aquatic animal locomotion. The philosophy of the immersed boundary method is that the elastic material is treated as a part of the fluid in which singular forces are applied. The fluid and the elastic immersed boundary constitute a coupled mechanical system: the motion of the fluid is influenced by the force generated by the immersed boundary on the fluid, but at the same time the immersed boundary moves at the local fluid velocity. The strength of this method is that it can handle the complicated and time dependent geometry of the elastic immersed boundary that interacts with the fluid, and that it does so while using a fixed regular lattice for the fluid computation.

Consider a viscous incompressible fluid which fills a periodic rectangular box $\boldsymbol{W}$ and an immersed boundary S, which is contained in the box. We shall now consider the mathematical formulation of the equations of motion for the fluid-immersed boundary system. The equations of motion are as follows:

$$\rho(\partial \mathbf{u}(\mathbf{x},t)/\partial t + (\mathbf{u}(\mathbf{x},t)\cdot\nabla)\mathbf{u}(\mathbf{x},t)) + \nabla p(\mathbf{x},t) = \mu\nabla^2\mathbf{u}(\mathbf{x},t) + \mathbf{F}(\mathbf{x},t) \quad (1)$$

$$\nabla\cdot\mathbf{u}(\mathbf{x},t) = 0 \quad (2)$$

$$\mathbf{F}(\mathbf{x},t) = f_S\, \mathbf{f}(s,t)\, \delta^2(\mathbf{x} - \mathbf{X}(s,t))\, ds \quad (3)$$

$$\mathbf{U}(s,t) = f_W\, \mathbf{u}(\mathbf{x},t)\, \delta^2(\mathbf{x} - \mathbf{X}(s,t))\, d\mathbf{x} \quad (4)$$

$$\partial\mathbf{X}(s,t)/\partial t = \mathbf{U}(s,t) \quad (5)$$

$$\mathbf{f}(s,t) = -\kappa_1(\mathbf{X}(s,t) - \mathbf{Z}(s,t)) + \kappa_2(\partial^2\mathbf{X}(s,t)/\partial s^2) \quad (6)$$

Equations 1 and 2 are the fluid (Navier-Stokes) equations, in Eulerian form. The fluid velocity $\mathbf{u}(\mathbf{x},t)$, the fluid pressure $p(\mathbf{x},t)$, and the singular force density $\mathbf{F}(\mathbf{x},t)$ are unknown functions of $(\mathbf{x},t)$, where $\mathbf{x} = (x,y)$ are fixed Cartesian coordinates and t is the time. Equations 3 and 4 are the interaction equations in mixed Eulerian and Lagrangian form. The core of the immersed boundary method is the delta function, which describes the interaction between the fluid and the immersed boundary. Equations 4 and 5 are, in effect, the no-slip condition, since they state that the immersed boundary moves at the local fluid velocity. Equations 5 and 6 are the immersed boundary equations in Lagrangian form. The configuration of the immersed boundary is described by the unknown function $\mathbf{X}(s,t)$, and $\mathbf{Z}(s,t)$ is the target position of the immersed boundary, which provides a restoring force that keeps the boundary points near their target positions, where $0 < s < L$ and L is the unstressed length of the immersed boundary. The force density $\boldsymbol{f}(s,t)$ and the velocity on the immersed boundary $\mathbf{U}(s,t)$ are also unknown functions of (s,t). A fixed value of the Lagrangian parameter s marks a material point of the immersed boundary. κ_1 and κ_2 are stiffness constants.

1.2. Numerical method. We present the summary of the immersed boundary method to find a numerical solution to the system of Equations 1-6. We impose periodic conditions on the computational rectangular domain. Our goal is to compute the update $\mathbf{u}^{n+1}$, $\mathbf{X}^{n+1}$ from given $\mathbf{u}^n$, $\mathbf{X}^n$. This is done in the following steps:

Step 1: Find the force $\mathbf{f}^n$ on the immersed boundary from the given boundary configuration $\mathbf{X}^n$.

Step 2: Spread the boundary force into the nearby lattice points of the fluid using the delta function.

Step 3: Solve the Navier-Stokes equations on the rectangular lattice to get the update $\mathbf{u}^{n+1}$ and p^{n+1} from $\mathbf{u}^n$ and $\mathbf{F}^n$. These equations are solved by the implicit first order scheme in time and space. The upwind scheme for the convection terms and the backward Euler differencing for the Stokes system are chosen. Because of the periodic boundary conditions of the computational domain, it is natural to use the Fast Fourier Transform (FFT) algorithm to solve equations for the unknowns $\mathbf{u}^{n+1}$ and p^{n+1}.

Step 4: Once the updated fluid velocity, $\mathbf{u}^{n+1}$ has been determined, we can find the velocity $\mathbf{U}^{n+1}$ and then the new position, $\mathbf{X}^{n+1}$ of the immersed boundary points.

This completes the description of the process (***Steps 1-4***, above) by which the quantities $\mathbf{u}$ and $\mathbf{X}$ are updated.

2. Two-Dimensional Model of Valveless Pumping

2.1.Initial position. Consider an incompressible viscous fluid with a constant density ρ and viscosity μ in a periodic rectangular box, which contains an immersed elastic boundary. Figure 1 shows the initial configuration of the immersed boundary in the form of a racetrack of 2-D valveless pumping in our numerical experiments. In this paper, we assume that the motions are driven by periodic vertical oscillations of the left 1/3 of the flexible tube boundary.

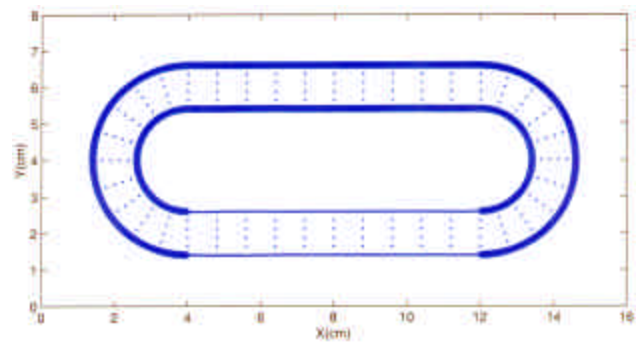

Figure 1. Initial position: flexible boundary (thin lines), almost rigid (thick lines), and fluid markers (dots).

2.2. Target positions and parameters. Recall that the equation for the force on the immersed boundary (Equation 6) involves target positions $\mathbf{Z}(s,t)$. For most of the flow loop, these are independent of time and serve the purpose of maintaining the racetrack shape of the flow loop. Time dependent target positions are used in the left 1/3 of the flexible segment of the flow loop (as shown in Figure 2) in order to provide periodic forcing to the flow. Figure 2 displays the target positions at eight equally spaced times over one cycle.

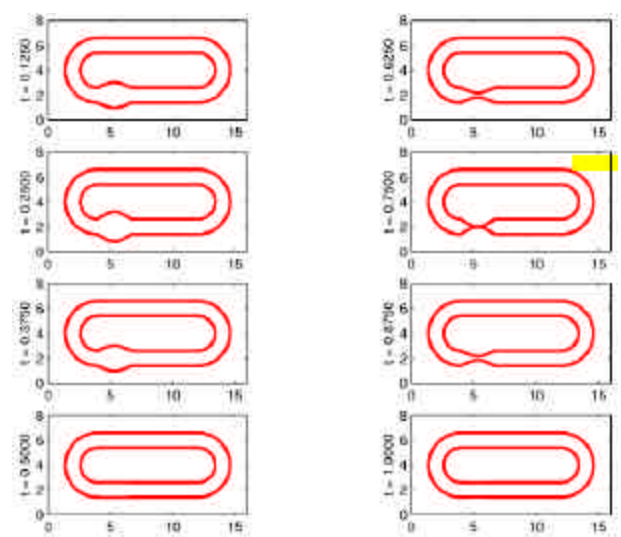

Figure 2. Target positions during one cycle.

In this work, we use CGS units. Tables 1 and 2 display the physical and computational parameters, respectively.

Physical parameters	Symbol	
Density	ρ	1 g/cm²
Viscosity	μ	0.01 g/cm· s
Diameter of tube	D	1.2 cm
Computational domain	X x Y	16 cm x 8 cm
Period	T	0.05 s ~ 4 s
Amplitude(target)	A_0	0.4 cm , 0.6 cm
Duration(experiment)	t_{max}	150 s

Table 1. Physical parameters

Computational parameters	Symbol	
Fluid lattice	N_x x N_y	256 x 128
Meshwidth	$h = \Delta x = \Delta y$	0.0625 cm
Initial distance between boundary points	$\Delta s = h/4$	0.0156 cm
Timestep duration	$\Delta t = 0.5\ h^2$	0.00195 s

Table 2. Computational parameters

3. Results and Discussion

There are two main results in this paper. First, a net flow around the loop is produced by the periodic forcing on one end of the flexible boundary, despite the absence of valves. Previous investigators have observed this phenomenon in physical experiments, and a theoretical explanation based on a lumped parameter (ODE) model has been proposed [5]. However, this is the first time, to our knowledge, that valveless pumping has been demonstrated by a computer simulation based on the Navier-Stokes equations. Second, we find that the direction of flow around the loop is determined not only by the position of the periodic compression, but also by the amplitude and frequency of the driving force. This is a new, unexpected phenomenon, not previously reported, and the most important prediction of our model.

In this section, we first justify our numerical method and then show that the amplitude and the frequency are the crucial parameters to determine the direction of a net flow around the loop.

3.1.Numerical convergence. To test the accuracy of our numerical scheme, we perform the same computation on the successive lattice refinements (128x64, 256x128, and 512x256) and compare the results in the L_2 norm. In Table 3, the parameters of this computation are as follows: period = 1.55 s, amplitude of the target position = 0.6 cm, and number of cycles = 96. The other physical parameters are the same as ones in Table 1. Since the asymptotic ratio is almost 2, our numerical method has almost first order accuracy.

$\| u_{64} - u_{128} \|_2 / \| u_{128} - u_{256} \|_2$	1.910726
$\| u_{128} - u_{256} \|_2 / \| u_{256} - u_{512} \|_2$	1.995359
$\| v_{64} - v_{128} \|_2 / \| v_{128} - v_{256} \|_2$	1.662576
$\| v_{126} - v_{256} \|_2 / \| v_{256} - v_{512} \|_2$	1.869106

Table 3. The ratio of the L_2 difference of velocities, **u**=(u,v)

3.2.The time-averaged flow around the loop as a function of the amplitude of the driving oscillation. We investigate the influence of the amplitude of the driving oscillation (i.e., the amplitude of the prescribed target position motion) on the magnitude and direction of the net flow around the loop of simulated tubing. Four different periods of the driving oscillation are considered: T = 0.3 s, 0.375 s, 0.525 s, and 1.7 s. Figure 3 displays the time-averaged flux as a function of the amplitude of the driving oscillation at these four chosen periods. Parameters other than amplitude and period are given in Tables 1 and 2. Positive flow values denote clockwise net flow and negative values denote counterclockwise net flow. The results plotted in Figure 3 show the following features:

- At low amplitude of the driving oscillation, net flow is always in the counterclockwise direction. Its magnitude at any given amplitude depends on the period of the driving oscillation. Of the four examples given in the figure, the periods T = 0.375 s and T = 1.7 s result in only weak counterclockwise flow; whereas, T = 0.3 s and T = 0.525 s result in much stronger counterclockwise flow.
- As the amplitude increases a qualitative distinction between the different cases appears. For T = 0.525 s and T = 1.7 s, the counterclockwise flow simply gets stronger monotonically as the amplitude of the driving oscillation increases. But for T = 0.3 s and for T = 0.375 s, the flow changes direction at some critical amplitude and becomes clockwise at high amplitude. Note that one cannot predict from the strength of the counterclockwise flow at low amplitude which of the cases will have clockwise flow at high amplitude.

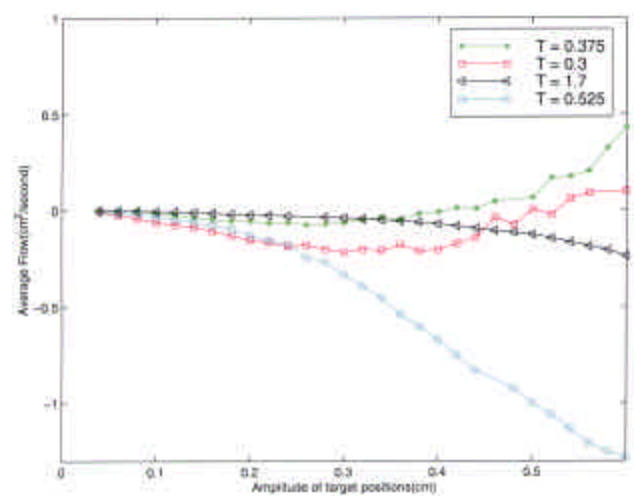

Figure 3. Time-averaged flux vs. Amplitude.

--

is that valveless pumping has a strong dependence on the frequency of the driving oscillation. Indeed, there appear to be resonances at rather specific frequencies, which are most effective in driving the flow in one direction or the other. At the lower amplitude, the net flow is almost always counterclockwise, so these peaks are in the negative direction. As we shift to the higher amplitude, the negative peaks seem to be preserved, but now positive peaks emerge as well. Another indication of the dynamic character of valveless pumping is that it seems to disappear at the extremes of frequency, the net flow approaches zero. In any case, strong valveless pumping happens at specific frequencies that are neither too large nor too small. The maximum net flow are generated at periods, T = 0.325 s (clockwise flow), and T = 0.21 s (counterclockwise flow) in the amplitude of the driving oscillation, A_0 =0.6 cm.

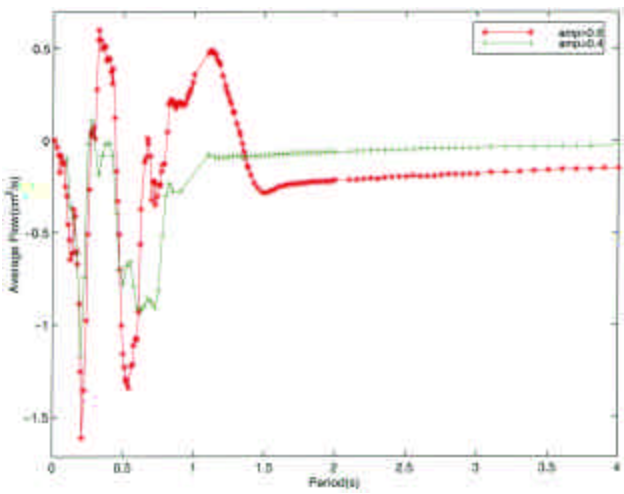

Figure 4. Time-averaged flux vs. Period (1/Frequency).

4. Conclusions

We have presented numerical experiments of "valveless pumping" in the two-dimensional case using the Immersed Boundary Method. As in the earlier papers and physical experiments of valveless pumping, we have also observed the existence of a net flow. Furthermore, we have presented the new, unexpected results that the direction of the flow around the loop of tubing is decided not only by the position of the driving oscillations, but also by the *frequency* and the *amplitude* of the driving oscillations. Since cardiopulmonary resuscitation (CPR) may involve valveless pumping, it is of obvious importance to know what fequency and amplitude of chest compression will produce the most effective CPR. Of course we cannot hope to answer this question quantitatively with such an idealized model, but perhaps we have shown qualitatively what phenomena may be expected as the frequency and amplitude of the driving oscillation are varied.

The immersed boundary methodology used here may also be applicable to other biological instances of valveless pumping, such as the blood circulation within the human embryo at the end of the third week of gestation, and to engineering applications such as the design of microelectromechanical system (MEMS).

We are confident that numerical experiments such as those begun in this paper will help answer many questions about the mechanism of valveless pumping. Even though these results demonstrate success in modeling valveless pumping, there is still much future work remains to be done. One avenue of research is giving a theoretical explanation for this mysterious phenomenon, and another is extending this model to the three-dimensional case in order to make it more realistic and more applicable real-world biomedical problems (e.g., CPR).

ACKNOWLEDGMENTS

This work was sponsored by the National Science Foundation (grant DMS-9626104) and by the U.S. Department of Energy, Assistant Secretary for Science, Office of Computational and Technology Research, Applied Mathematical Sciences Program, under contract DE-AC05-96OR22464 with Lockheed Martin Energy Research Corporation. Oak Ridge National Laboratory is managed by Lockheed Martin Energy Research Corporation for the United States Department of Energy under Contract No. DE-AC05-96OR22464. Computation was performed in part at NYU's Applied Mathematics Laboratory and in part at the San Diego Supercomputer Center through a grant from the National Research Allocations Committee (MCA93S004).

This submitted manuscript has been authored by a contractor of the U.S. Government under Contract No. DE-AC05-96OR22464. Accordingly, the U.S. Government retains a nonexclusive, royalty-free license to publish or reproduce the published form of this contribution, or allow others to do so, for U.S. Government purposes.

REFERENCES

[1] Criley, J. M., Niemann, J. T., Rosborough, J. P., Ung, S., and Suzuki, J. The heart is a conduit in CPR. *Crit. Care Med*., 9:373, 1981.

[2] Feneley, M. P.. M.D., F.R.A.C.P., George W. Maier, M.D., J. William Gaynor, M.D., Stanley A. Gall, B.S., Joseph A. Kisslo, M.D., James W. Davis, M.S.E.E., and J. Scott Rankin, M.D. Sequence of mitral valve motion and transmitral blood flow during manual cardiopulmonary resuscitation in dogs. *Circulation,* 76, No. 2:363-375, 1987.

[3] Kilner, P. Formed flow, fluid oscillation and the heart as a morphodynamic pump. *Royal Brompton Hospital.*

[4] Miyazaki, S., Kawai, T., and Araragi, M. A piezo-electric pump driven by a flexural progressive wave. IEEE Transactions, 282-288, 1991.

[5] Moser, M., Huang, J. w., Schwarz, G. S. Kenner, T., and Noodergraaf, A. Impedance defined flow, generalization of William Harvey's concept of the circulation – 370 years later. *International Journal of Cardiovascular Medicine and Science,* 71:205-211, 1998.

[6] Peskin, C. S. and McQueen D. M. A general method for the computer simulation of biological systems interacting with fluids. *Symposia of the Society for Experimental Biology*, 49:265-276, 1995.

[7] Peskin, C. S. and McQueen D. M. Fluid dynamics of the heart and its valves. Case studies in mathematical modeling – Ecology, Physiology, and Cell Biology, 309-337, 1996.